ROLLING MOSAIC METHOD TO SUPPORT THE DEVELOPMENT OF POTENTIAL FISHING ZONE FORECASTING FOR COASTAL AREAS

Komang Iwan Suniada[1]*, Eko Susilo, Wingking Era Rintaka Siwi, Nuryani Widagti
[1]Institute for Marine Research and Observation, Jembrana, Bali, Indonesia
*email: komang.prtk@gmail.com
Received: 25 November 2019; Revised: 13 February 2020; Approved: 13 February 2020

Abstract. The production of the Indonesian Institute for Marine Research and Observation's mapping of forecast fishing areas (*peta prakiraan daerah penangkapan ikan* or PPDPI) based on passive satellite imagery is often constrained by high-cloud-cover issues, which lead to sub-optimal results. This study examines the use of the rolling mosaic method for providing geophysical variables, in particular, sea-surface temperature (STT) together with minimum cloud cover, to enable clearer identification of oceanographic conditions. The analysis was carried out in contrasting seasons: dry season in July 2018 and rainy season in December 2018. In general, the rolling mosaic method is able to reduce cloud cover for sea-surface temperature (SST) data. A longer time range will increase the coverage percentage (CP) of SST data. In July, the CP of SST data increased significantly, from 15.3 % to 30.29% for the reference 1D mosaic and up to 84.19 % to 89.07% for the 14D mosaic. In contrast, the CP of SST data in December tended to be lower, from 4.93 % to 13.03% in the 1D mosaic to 41.48 % to 51.60% in the14D mosaic. However, the longer time range decreases the relationship between the reference SST data and rolling mosaic method data. A strong relationship lies between the 1D mosaic and 3D mosaics, with correlation coefficients of 0.984 for July and 0.945 for December. Furthermore, a longer time range will decrease root mean square error (RMSE) values. In July, RMSE decreased from 0.288°C (3D mosaic) to 0.471°C (14D mosaic). The RMSE value in December decreased from 0.387°C (3D mosaic) to 0.477°C (14D mosaic). Based on scoring analysis of CP, correlation coefficient and RMSE value, results indicate that the 7D mosaic method is useful for providing low-cloud-coverage SST data for PPDPI production in the dry season, while the 14D mosaic method is suitable for the rainy season.

Keywords: *rolling mosaic, potential fishing zone forecast, coastal area, SST, cloud cover.*

1 INTRODUCTION

Peta Prakiraan Daerah Penangkapan Ikan (PPPDI) [Mapping Of Forecast Fishing Areas] is a key product of the Institute for Marine Research and Observation (IMRO) of Indonesia, aimed at supporting fishers in determining fishing locations. PPDPI contains information at both national and coastal scale and for particular fish species. Several studies have been carried out to improve the accuracy of PPDPI and the results indicate that fish catches tend to increase when fishing activities are conducted in areas closer to locations indicated on PPDPI (Yunanto & Suniada, 2008). Pertami and Suniada (2014) conclude that the average level of accuracy of PPDPI in the Bali Strait was 41.80% in 2013, with the highest level of accuracy, of 69.57%, occurring in October. Besides using fishing data, the level of accuracy of PPDPI is assessed by using data for micronekton abundance (Susilo & Suniada, 2015) and fishing-vessel distribution data from radar satellites (Hastuti, Suniada, Susilo, & Saputra, 2016). A study of fishing-vessel

http://dx.doi.org/10.30536/j.ijreses.2019.v16.a3252

distribution in the Fisheries Management Area, Republic of Indonesia 711 (FMA-RI 711) related to PPDPI shows that the highest accuracy, of 87%, occurred in May (Hastuti et al., 2016).

PPDPI is produced by utilizing geophysical variables such as sea-surface temperature (SST) and chlorophyll-a concentration (chl_a) derived from satellite imagery. The satellite imagery data currently used comes from the Aqua/Terra satellite's MODIS (MODerate-resolution Imaging Spectroradiometer) sensor. The national-scale map is produced using level-3 data at 4 km spatial resolution. In order to obtain more detailed information for smaller-scale areas such as coastal-scale mapping, higher resolution of Aqua/Terra MODIS data is required. Operationally, coastal-scale maps are generated every day using daily level-2 Aqua/Terra MODIS products with spatial resolution of 1 km.

MODIS is classified as a passive sensor that utilizes solar radiation illuminating the earth's surface, detecting reflection from the surface (Zhu et al., 2018). Information may not be received by the sensor if the earth's surface is obstructed by clouds. Hence, cloud cover is the main issue in obtaining geophysical variables from satellites which employ passive sensors. Furthermore, coastal-scale maps cannot be produced if the satellite data reveals high cloud coverage, as is the case particularly in the rainy season.

The Indonesian area is characterized by high cloud coverage in the rainy season and this generates a significant decrease in the number of coastal-scale maps produced. As cloud coverage starts to decrease in the dry season so PPDPI production increases (Figure 1-1).On average, the percentage of coastal-scale map production during the period January to September 2018 is only around 16.01%.

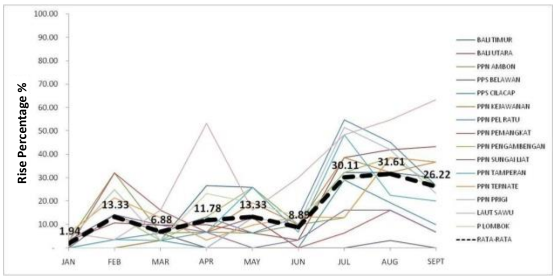

Figure 1-1: Percentage of coastal-scale map production from January–September 2018.

This low percentage of coastal-scale map production and the high cloud coverage typical in the Indonesia area has led to research into methods which could be used to obtain SST data with minimum cloud coverage. Several studies seeking to produce cloud-free data have been conducted, such as He, Weisberg, Zhang, Muller-Karger, & Helber (2003) who combined AVHRR data with TMI data using the optimum interpolation (OI) approach. Sirjacobs, Weisberg, Zhang, Muller-Karger, & Helber (2011) attempted to fill in the total suspended matter data – chl_a, and SST data that was missing – by using the data interpolating empirical orthogonal functions (DINEOF) method. Meanwhile, Jatisworo, Murdimanto, Kusuma, Sukresno, & Berlianty (2018) used the gap-filling method using MUR-SST data and Himawari-8 data to fill in SST lost because of cloud cover. Most of the studies carried out to produce cloud-free data use fairly complex processes that consist of various kinds of input data and methods; however, for operational activities a simpler process is required that uses only a single input.

The aim of this study is to compile a prototype of SST with minimum cloud coverage derived from satellite imagery by using a rolling mosaic method for single sensor data (i.e. MODIS) with a multi-temporal scale comprising data in a certain time range. The final result of this study is expected to reduce the effect of cloud coverage to at least 50% to support the development of coastal PPDPI, particularly in increasing the number of coastal-scale maps produced.

2 MATERIALS AND METHODOLOGY

2.1 Location and data

The study area covers all Indonesian waters from 92°E – 141°E and 7°N – 11°S. The SST imagery analysed in this study was acquired from the MODIS sensor onboard the Aqua/Terra satellite. The daily level-2 SST products with 1 km spatial resolution were downloaded from the OceanColor server in ncdf format. It takes four to six scenes to cover the study area, and the satellites have a revisit time of 16 days, meaning it will acquire data for the same place at the same time every 16 days.

The analysis was performed for contrasting dry and rainy seasons. Daily data for July 2018, which has minimum cloud coverage, was chosen to represent the dry season. A total of 109 scenes were chosen from 11 to 31 July 2018. The rainy season, which usually has high cloud coverage, was represented by daily data from December 2018. A total of 105 scenes were chosen from 11 to 31 December 2018.

2.2 SST data processing

SST data processing was performed using Sentinel Application Platform (SNAP) open-source data-processing software, which can be downloaded free from the ESA website (http://step.esa.int/main/toolboxes/snap/).

In general, SST data processing consists of several stages. The first step is quality filtering for each pixel value based on certain criteria. The SST level-2 product is accompanied by masking criteria information used to characterize the quality of each retrieved pixel value. This information is stored in the qual_sst band. Quality level-0 is the highest quality while level-4 is the worst quality (Table 2-1). Quality levels-0 and level-1 were chosen for further SST processing. These two quality levels show the best pixel quality based on satellite angle and the reflection of the sun or cloud coverage. We excluded quality levels-2 to level-4 by using the following equation:

$$\text{if qual\_sst}>1 \text{ then NaN else SST} \qquad (2\text{-}1)$$

This simple equation implies that if the qual_sst value is more than 1 then the SST will be changed to NaN (without value). Otherwise, if the qual_sst value is 0 or 1 then the pixel value will be allocated according to the SST value of that pixel.

Then, the filtered SST product is reprojected, this being the process for changing or adding coordinate information (longitude/latitude) to satellite imagery data. The coordinate reference system commonly used in Indonesia is geographic long/lat (WGS 84).

Table 2-1: Quality level definitions for daily level-2 SST products.

Quality level	Meaning
0	Best satellite zenith angle < 55 degrees
1	Good/acceptable in glint or high viewing angle
2	Suspect
3	Bad cloud/ice/dust or atmospheric correction failed
4	Not processed or land

A							
Date	22	23	24	25	26		and so on....
	22	23	24	25	26		
	22	23	24	25	26		

B											
Date	18	19	20	21	22	23	24	25	26		and so on....
	18	19	20	21	22	23	24	25	26		
	18	19	20	21	22	23	24	25	26		

C																	
Date	11	12	13	14	15	16	17	18	19	20	21	22	23	24	25	26	and so on....
	11	12	13	14	15	16	17	18	19	20	21	22	23	24	25	26	
	11	12	13	14	15	16	17	18	19	20	21	22	23	24	25	26	

Figure 2-1: Rolling mosaicing procedures (A: 3D mosaic; B: 7D mosaic; C: 14D mosaic)

2.3 Rolling mosaicing procedure

Mosaicing is the process of combining several items of satellite image data into one single image. This study uses several rolling mosaics, including daily (1D mosaic), rolling 3-day (3D mosaic), rolling 7-day (7D mosaic) and rolling 14-day (14D mosaic) data. These procedures are almost the same as those used for calculating the moving average.

The 3D mosaic is described in Figure 2-1A. STT data for the 24th is produced from a combination of three days of SST dataset, for the 22nd to the 24th. Similarly, the SST data for the 25th is produced by combining the 23rd, 24th and 25th SST data and the SST data for the 26th by combining the 24th, 25th and 26th SST data, and so on. The same procedure is applied for the 7D mosaic (Figure 2-1B) and the 14D mosaic (Figure 2-1C). In summary, the 3D mosaic is arranged using data with a time range of 3 days, 7D mosaic with a time range of 7 days, and 14D mosaic with a time range of 14 days.

2.4 CP analysis

The coverage percentage (CP) refers to the cloud-free coverage area. CP was calculated based on the ratio between the numbers of pixels that contain SST values and the number of pixels in the sea. The study area, which lies from 92°–141°E to 7°N–11°S, is composed of 8,820,000 pixels (4,800 x 1,900). While the number of land pixels, referring to quality level information (Table 2-1), was 1,908,262 pixels, the number of pixels in the sea, calculated by subtracting the total pixels and land pixels, was 6,911,738.

$$CP = \frac{n_{SST}}{n_{sea}} \, x \, 100\% CP = \frac{n_{SST}}{n_{sea}} \, x \, 100\% \quad (2\text{-}2)$$

n_{SST} = number of pixels that contain SST value; n_{sea} = number of pixels in the sea (6,911,738).

2.3 Correlation analysis

Correlation analysis was conducted to determine the strength of the relationship between the rolling mosaics and the reference dataset. The 1D mosaic SST data was chosen as the reference dataset and the 3D, 7D and 14D mosaic SST data as predictive datasets. In this study, 500 sampling points were chosen randomly around the study area (Figure 2-2). The process analysis was carried out using the open-source software Quantum GIS. Pearson correlation analysis and scatter diagrams (Walpole, 1993) were used to compare all datasets.

$$r = \frac{n\sum x_i y_i - \sum x_i \sum y_i}{\sqrt{n\sum x_i^2 - (\sum x_i)^2} - \sqrt{n\sum y_i^2 - (\sum y_i)^2}} \quad (2\text{-}3)$$

where n = number of data (500 points), x = reference dataset (daily mosaic), y = rolling mosaic datasets (3D mosaic, 7D mosaic and 14D mosaic).

In addition, root mean square error (RMSE) was calculated to determine the error for each rolling mosaic method compared to the random reference dataset at different times and places. The smaller the RMSE value indicate the better the performance of the rolling mosaic methods (Widayati, 2009). According to Chai and Draxler (2014), the RMSE can be calculated using the following equation (Equation 4):

$$RMSE = \sqrt{\frac{1}{n}\sum_{i=1}^{n} e_i^2} \quad (2\text{-}4)$$

2.3 Scoring analysis

Scoring analysis was conducted to find out the most suitable among the rolling mosaic methods for producing SST data with minimum cloud coverage. This scoring analysis consists of weights and scores based on certain parameters and criteria (Table 2-2), including:

1. RMSE value was given the highest weight of 0.4 because the error rate is the most important factor in the process of making predictions.
2. CP was given weight of 0.35 to ensure that cloud coverage is seen as important and given the second highest weight. Given the aim of this study, rolling mosaics with CP of less than 50% are excluded from the scoring analysis.
3. Pearson correlation was given a weight of 0.25 because, although it is an important parameter in knowing the direction and strength of the relationship between the reference value and the predicted value, its priority is slightly lower than the percentage parameter for cloud cover.

The highest value obtained from the scoring analysis is considered as a suitable method for producing cloud-free SSTdata.

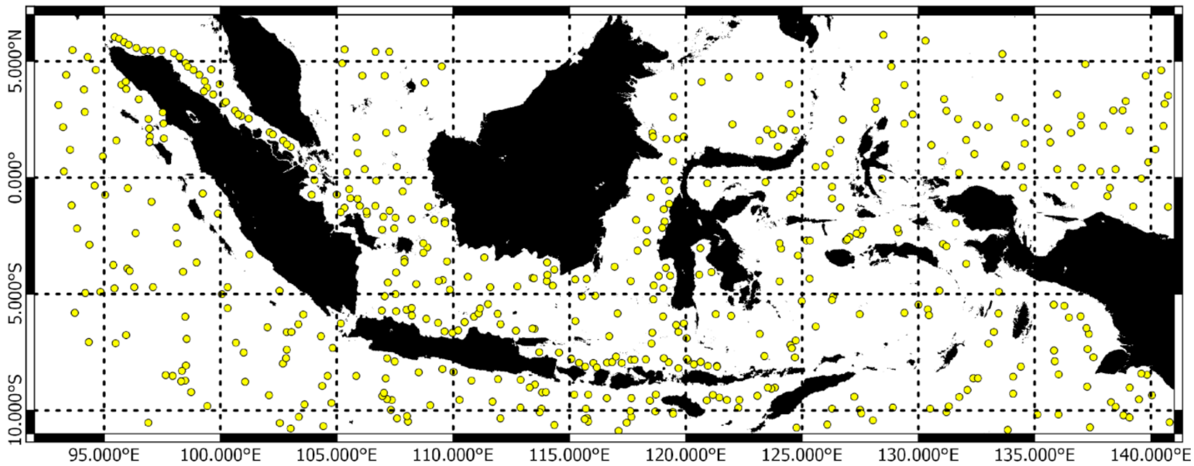

Figure 2-2: Spatial distribution of 500 random sampling point datasets

Table 2-2: Weights and scores criteria

	RMSE	Coverage percentage (CP)	Pearson correlation
Weight	0.4	0.35	0.25
Score			
1	>0.4	50 – 60	<0.6
2	0.3 – 0.4	61 – 70	0.61 – 0.7
3	0.2 – 0.3	71 – 80	0.71 – 0.8
4	0.1 – 0.2	81 – 90	0.81 – 0.9
5	<0.1	>91	>0.91

3 RESULTS AND DISCUSSION

3.1 Filtered SST

SST level-2 product was accompanied by masking criteria information used to characterize the quality of each retrieved pixel value stored in the qual_sst band. Quality level values of 0 and 1 were chosen for further processing. The filtering process is illustrated in Figure 3-1 for SST data acquired on 1 July 2018. This image consists of 2,088,129 unfiltered SST pixels (Figure 3-1A). Based on the masking criteria, only 580,490 pixels (about 28%) meet the best quality criteria. This means that 1,507,638 pixels (72%) are low-quality and should be ignored for further processing.

The number of low-quality pixels that will be ignored due to the filtering process differs between data sets depending on atmospheric conditions, the position of the satellite angle when recording and the cloud-detection algorithm used (Koner & Harris, 2016). Atmospheric conditions, especially clouds, are major obstacles when using passive sensors for monitoring land and sea conditions. However, in the field of weather monitoring, cloud cover is also very important because it is the main indicator in determining the weather conditions at a particular place (Sudiana, 2009). In this study, filtered SST will be used for the rolling mosaic process.

3.2 Dry season SST

A total of 109 scenes were analysed to represent the dry season. Based on the CP values, the analysis shows that the rolling mosaic method works well during the dry season and increases the percentage of data by up to 89%, reducing the percentage of cloud cover obtained.

The 1D mosaic data from 24-31 July 2018 has the lowest CP range, of between 15.3% and 30.29%. Meanwhile, 3D and 7D mosaic data have higher CP value ranges, of 46% to 56.75% and 72.24% to 77.88%, respectively. The 14D mosaic has the highest CP value range, of 84.19% to 89.07%. The CP value for each rolling mosaic can be seen in Figure 3-2.

Increasing the time range used leads to an increasing amount of data being used to compile each mosaic, thus producing higher CP. From the different rolling mosaic distributions, the spatial distribution of filtered SST data for 24 July 2018 reveals an increase in CP value and a decrease in cloud coverage (Figure 3-3). In Figure 3-3, image A was obtained from the 1D mosaic. Using the 3D mosaic based on SST data from July 22–24 2018 we can clearly produce SST data for the Natuna Sea, Java Sea and Indian Ocean. Further, by using the 7D mosaic based on SST data from 18–24 July and the 14D mosaic based on SST data from 11–24 July, we can produce SST data which covers almost the whole study area.

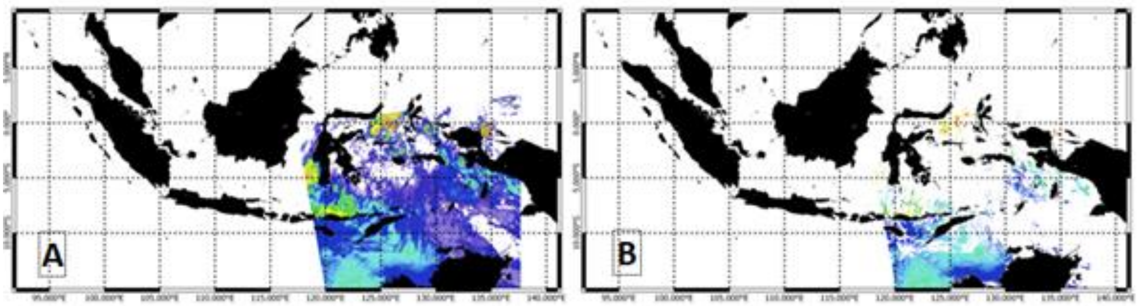

Figure 3-1: Data filtering process: A) before filtering; B) after filtering

The reduction in cloud coverage will enable the oceanographic characteristics of Indonesia's territorial waters to be more clearly illustrated and this can be seen from the results of the 3D mosaic SST data (Figure 3-3). The mosaic data shows that SSTs in South Java to Nusa Tenggara, Banda Sea, and Papua waters are blue, which indicates cooler temperatures. This is consistent with the results of research by Hendiarti et al., (2005). During the southeast monsoon, there is intensive wind stress that will lead surface water masses to move southward. This water-mass movement will cause a vacuum in the surface layer and which will quickly be replaced by subsurface water masses. This process of increasing water mass from the lower layer which has a lower temperature but is rich in nutrients is known as upwelling. Rintaka and Susilo (2015) state that the southeast monsoon is very closely related to the Ekman upwelling process that occurs along the southern coast of Java, from Bali-Nusa Tenggara to the Banda Sea, a process that will cause a decrease in SST in this area. This is caused by strong gusts of wind which cause vertical mixing of surface layer water with the subsurface layer, which is relatively cooler (Susanto, Moore, & Marra, 2006). These upwelling phenomena and changes in SST can be clearly observed using satellite data (Hendiarti, Siegel, & Ohde, 2004).

To ascertain the distribution pattern of SST for each of the rolling mosaic methods, 500 random samples of SST were chosen for each day of SST data from 24–31 July 2018. From these, 1,177 samples were used to identify the distribution pattern of SST. All datasets show almost the same distribution pattern. In general, the SST range is between 24.035°C and 33.825°C (Figure 3-4).

This similar distribution pattern of SST may occur because of the strength of the relationship between the 1D mosaic and the other rolling mosaic results, as shown by the points of SST value being located close to the 45° trend line, as illustrated in Figure 3-5.

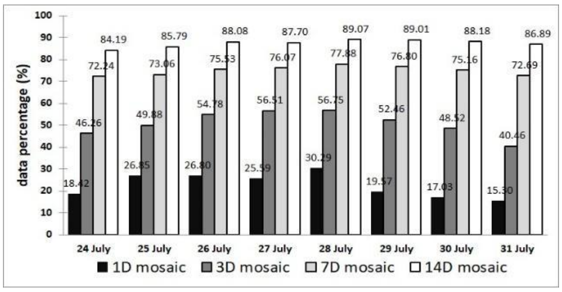

Figure 3-2: CP of SST data from July 24–31 2018

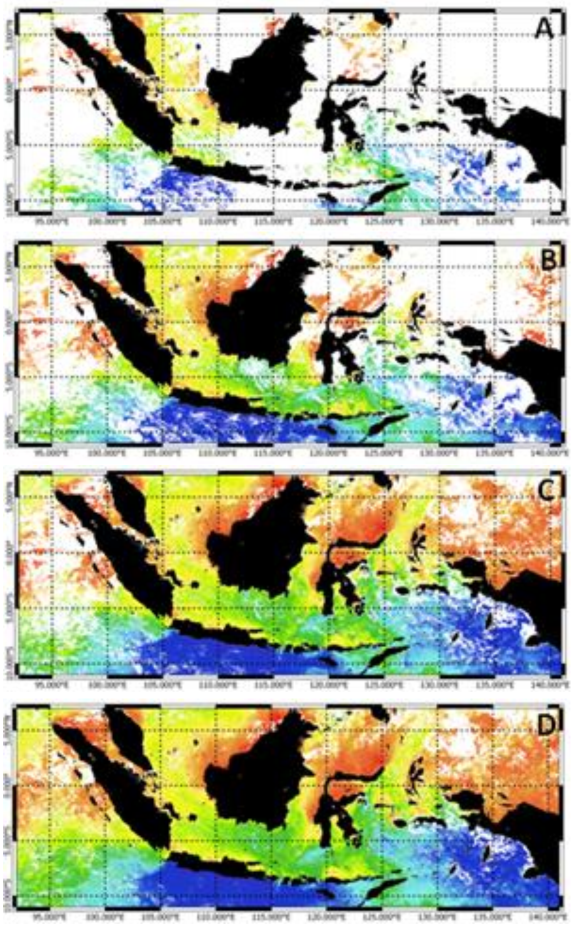

Figure 3-3: Spatial distribution of SST on 24 July 2018 (A: 1D mosaic; B: 3D mosaic; C: 7D mosaic; D: 14D mosaic)

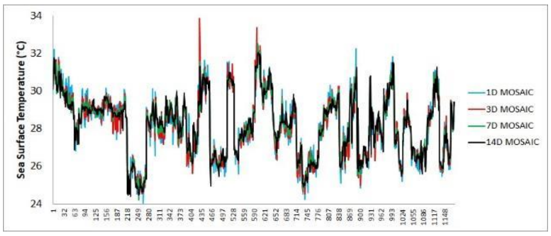

Figure 3-4: Distribution pattern of SST for each rolling mosaic method on 24 July 2018

The Pearson correlation value indicates a very strong, positive (unidirectional) relationship between the 1D mosaic and the 3D mosaic, with a correlation coefficient of 0.984 (R2 = 0.969). Also, there is a very close relationship between the 1D and 7D mosaics, with a correlation coefficient of 0.972 (R2 = 0.945). A very close relationship is also seen between the 1D and 14D mosaics, with a correlation coefficient of 0.959 (R2 = 0.919).

Even though the 1D mosaic has a close relationship with all the rolling mosaics, the strength of the relationship decreases with the increasing time range used to compile the mosaic. This is indicated by the highest correlation coefficient being for the 3-day range used to compile the 3D mosaic SST data. The correlation coefficient then decreases again for the 7-day range and yet further for the 14-day range.

In general, all of the rolling mosaics have the same distribution patterns with the same high levels of correlation. However, there is a small difference in SST values between each of the rolling mosaic methods. RMSE values show the 3D mosaic to have the smallest error and the closest value to the reference SST data (1D mosaic). The RMSE value between the 1D and 3D mosaics is 0.288°C, while the RMSE between the 1D and 7D mosaics is 0.388°C. The highest RMSE value is 0.471°C found between the 1D and 14D mosaic values.

The 1D mosaic and 3D mosaic SST data is dominated by intervals of between 0 and 0.1˚C, i.e. the 3D data is very close to the reference data. This difference from the 1D mosaic data increases significantly as the time range increases, with the difference between the reference and 14D mosaic values mostly being greater than 0.3°C (Figure 3-6).

Based on the scoring analysis, the 7D mosaic results have the highest total score, of 3.10. This means that the 7D mosaic has that best performance and is therefore suitable for producing cloud-free SST data in the dry season.

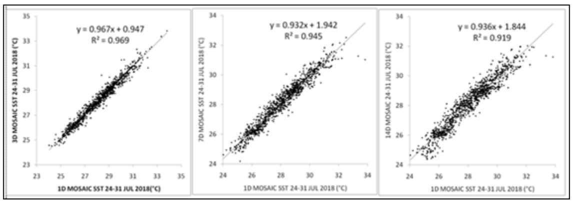

Figure 3-5. Scatter diagrams for reference SST data (1D mosaic) and other rolling mosaics for 24 July 2018

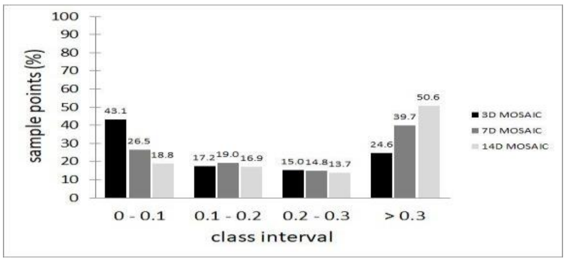

Figure 3-6: Interval classes of differences in SST values between 1D mosaic and each rolling mosaic for 24 July 2018

Table 3-1: Scoring summary for each rolling mosaic in the dry season

Criteria	Weight (W)	3D mosaic			7D mosaic			14D mosaic		
		Value (V)	Score (S)	W x S	Value (V)	Score (S)	W x S	Value (V)	Score (S)	W x S
RMSE	0.40	0.288	3	1.20	0.388	2	0.80	0.471	1	0.40
CP	0.35	57.75	1	0.35	77.88	3	1.05	89.07	4	1.40
Pearson correlation	0.25	0.984	5	1.25	0.972	5	1.25	0.959	5	1.25
Total score				2.80			3.10			3.05

3.3 Rainy season SST

A total of 105 scenes drawn from 11 to 31 December 2018 was analysed to represent the rainy season. Based on the CP values, it can be seen that the rolling mosaics give poorer results for the rainy season than for the dry season. This method only increases the percentage of data obtained to 51%, i.e. a lower increase than for the dry season.

The 1D mosaic data for 24 to 31 December 2018 has a lower CP range, of between 4.93% and 13.03%. The 3D mosaic and 7D mosaics have better CP value ranges, of 13.54% to 25.49% and 27.17% to 35.83%, respectively. The 14D mosaic has the highest CP values, ranging between 41.48% to and 51.60%. The CP values for each rolling mosaic can be seen in Figure 3-7. These results are consistent with those of Aldrian (2000), who stated that there was an increase in the intensity of rain in all of parts of the Indonesia region in December, as part of the cycle of the Asian monsoon which strengthens during this month.

The spatial distribution of SST data from all the rolling mosaics indicates that high cloud coverage masks the middle of the Indonesian archipelago. Moreover, there are still some areas where SST cannot be provided even using the 14D mosaic (Figure 3-8). High rainfall intensity is also significantly associated with this high cloud coverage, which in December meant the CP of SST data could not be significantly increased.

Randomly selected SST values during this time range indicate that SST is warmer than during the dry season period, ranging between 26.805°C and 33.825°C. The patterns of SST for all the rolling mosaics show the same distribution (Figure 3-9).

The scatter diagrams indicate that the rainy season SST distribution is more diffuse than, and slightly deviates from, the trend line of the dry season results. However, the correlation coefficients are still relatively high, thus indicating a strong and direct relationship to all mosaic data (Figure 3-10).

Based on the Pearson correlation value, there is a strong and positive relationship between the 1D and 3D mosaics, with a correlation coefficient of 0.945 (R2 = 0.893). A less strong relationship is found between the 1D and 7D mosaics and the 1D and 14D mosaics, with correlation coefficients of 0.878 (R2 = 0.771) and 0.803 (R2 = 0.645), respectively. Even though the correlation coefficients are lower than for the dry season, they indicate that a longer time range used to compile the mosaic data will still decrease the relationship between the SSTs drawn from reference data and the rolling mosaic data.

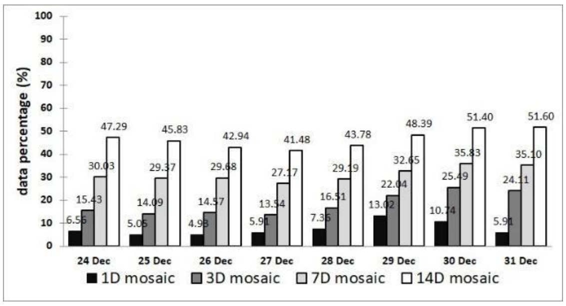

Figure 3-7: CP of SST data from 24–31 December 2018

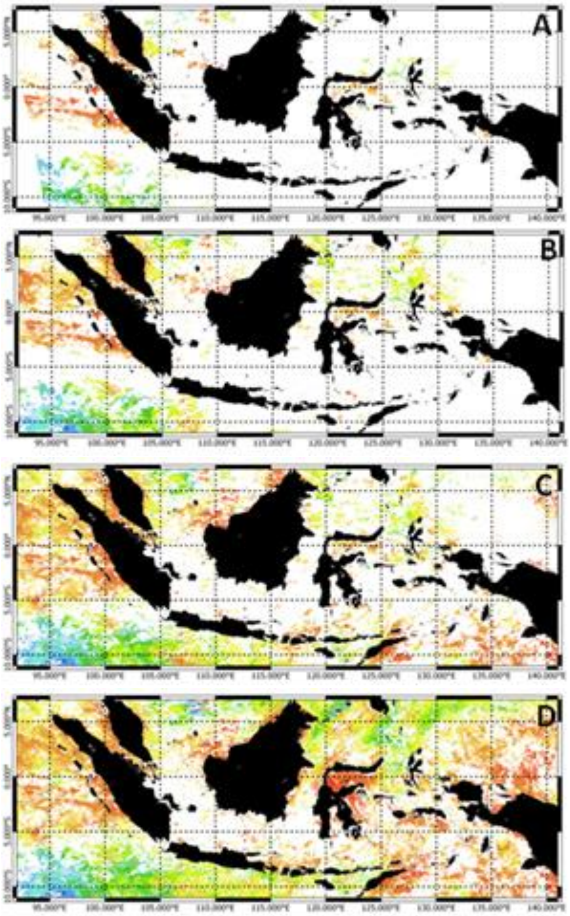

Figure 3-8: Spatial distribution of SST on 24 December 2019: A) 1D mosaic; B) 3D mosaic; C) 7D mosaic; D)14D mosaic

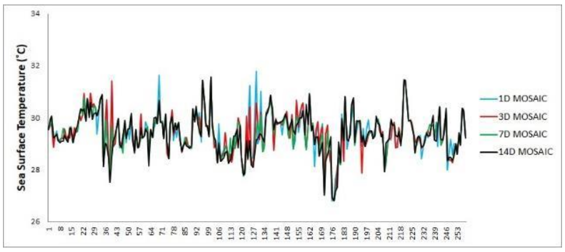

Figure 3-9: Distribution pattern of SSTs for each rolling mosaic methods for 24 December 2018

Furthermore, a longer time range used for the rolling mosaic process will affect the quality of the SST data, indicated by the difference in value from the reference data increasing. This is confirmed by higher RMSE values. The RMSE value between the 1D and 3D mosaics is 0.263°C while the RMSE value between the 1D and 7D mosaics is 0.387°C. The RMSE value between the 1D and 14D mosaic gives the highest value, of 0.477°C.

The difference in SST between the reference data (1D mosaic) and the rolling mosaics mostly lies between 0 and 0.1°C. More than 71.4% of the different SST values in the comparison of the 1D and 3D mosaic data are between 0 and 0.1°C. A similar lower percentage was also calculated between the 1D mosaic and the 7D and 14D mosaics, of 50.2% and 43.6%, respectively (Figure 3-11). Increasing time range leads to a decrease in the percentage of SST values in the internal 0 to 0.1°C, indicating that the 3D mosaic has the smallest error and can therefore be said to have a value closest to the reference data.

Finally, based on the scoring analysis, it is evident that the 14D mosaic method can provide a CP of more than 50%, while the other two methods give CP which is less than the minimum requirement. This means that the 14D mosaic is suitable for producing cloud-free SST data in the rainy season. However, the lower accuracy value and higher error (RMSE) produced remain issues still to be addressed.

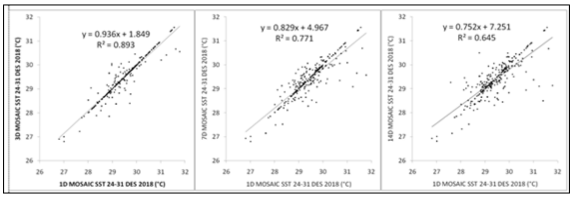

Figure 3-10: Scatter diagrams of comparisons of reference SST data (1D mosaic) and other rolling mosaics on 24 December 2018

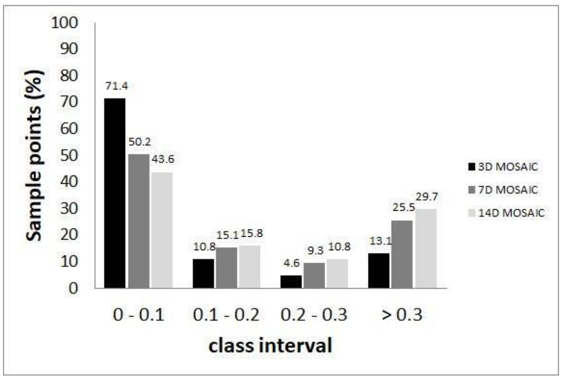

Figure 3-11. Interval classes of difference SST values between 1D mosaic and each rolling mosaic on 24 December 2018

Table 3-2: Scoring summary for each rolling mosaic in the rainy season

Criteria	Weight (W)	3D mosaic			7D mosaic			14D mosaic		
		Value (V)	Score (S)	W x S	Value (V)	Score (S)	W x S	Value (V)	Score (S)	W x S
RMSE	0.4	0.263	3	1.20	0.387	2	0.80	0.477	1	0.40
CP	0.35	25.49	1	0.35	35.83	1	0.35	51.60	1	0.35
Pearson correlation	0.25	0.945	5	1.25	0.878	4	1.00	0.803	3	0.75
	Total Score			2.80			2.15			1. 50

4 CONCLUSION

Rolling mosaic methods are able to reduce cloud coverage on SST data enabling it to clearly image oceanographic conditions in near-real time. The 7D mosaic method is suggested for use in routine production to increase the CP of SST data to support coastal-scale mapping, especially during the dry season. In contrast, the 14D mosaic is more suitable for use during the rainy season. In addition, the rolling mosaic method is the simplest method to run for SST datasets from the MODIS sensor for certain time ranges. Using low-cloud-coverage SST data, the production of coastal-scale mapping can be improved in accuracy and coverage area, as well as production time being reduced.

ACKNOWLEDGEMENTS

This study was funded in 2018 by the Ministry of Marine Affairs and Fisheries, the Republic of Indonesia, through the Institute for Marine Research and Observation (IMRO). The authors wish to thank the NASA Goddard Space Flight Centre-OBPG for providing free Aqua/Terra MODIS data. We also express appreciation to the journal editorial team and reviewer for their valuable comments, and thank the SINAS INDERAJA 2019 committee for awarding 'best presenter' to this paper.

AUTHOR CONTRIBUTIONS

Rolling Mosaic Method To Support The Development Of Potential Fishing Zone Forecasting For Coastal Areas. Lead Author: Komang Iwan Suniada; Co-Author: Eko Susilo, Wingking Era Rintaka Siwi, and Nuryani Widagti

REFERENCES

Aldrian, E. (2000). Pola hujan rata-rata bulanan wilayah Indonesia; tinjauan hasil kontur data penakar dengan resolusi Echam T-42 (Average monthly rainfall patterns in Indonesia: A review of the results of measuring pen contours with T-42 Echam resolution). *Jurnal Sains & Teknologi Modifikasi Cuaca 1*(2), 113–123.

Chai, T. & Draxler, R. R. (2014). Root mean square error (RMSE) or mean absolute error (MAE)? – Arguments against avoiding RMSE in the literature. *Journal of Geoscientific Model Development, 7*, 1247–1250.

Hastuti, A. W., Suniada, K. I., Susilo, E., & Saputra, A. J. (2016). Distribusi sebaran kapal ikan dan kaitannya dengan daerah potensial penangkapan ikan berdasarkan citra satelit di WPP-NRI 711 (The distribution of fishing vessels and its relationship with potential fishing grounds based on satellite imagery in Indonesian FMA 711). Prosiding Seminar Nasional Penginderaan Jauh LAPAN 2016.

He, R., Weisberg, R. H., Zhang, H., Muller-Karger, F. E., & Helber, R. W. (2003). A cloud-free, satellite-derived, sea surface temperature analysis for the West Florida Shelf. *Geophysical Research Letters*, *30*(15).

Hendiarti, N., Siegel, H., & Ohde, T. (2004). Investigation of different coastal processes in Indonesian water using SeaWiFS data. *Deep Sea Research Part II:Tropical Studies in Oceanography, 51*(1-3), 85–97.

Hendiarti, N., Suwarso, Aldrian, E., Amri, K., Andiastuti, R., Sachoemar, S. I., & Wahyono, I. B. (2005). Seasonal variation of pelagic fish catch around Java. *Oceanography 18*(4), 112–123.

Jatisworo, D., Murdimanto, A., Kusuma, D. W., Sukresno, B., & Berlianty, D. (2018). Analisis penerapan metode gap filling untuk optimalisasi peroleh data suhu permukaan laut bebas awan di Selat Bali (Analysis of the application gap filling method for optimization of cloud free sea surface temperature data in the Bali Strait). *Jurnal Penginderaan Jauh dan Pengolahan Citra Digital, 15*(2), 1–14.

Koner, P.K. & Harris, A. (2016). Improved quality of MODIS sea surface temperature retrieval and data coverage using physical deterministic methods. *Journal of Remote Sensing, 8*(454), 1–16.

Pertami N. D. & Suniada, K. I. (2014). Utilization of satellite remote sensing data for the determination of potential fishing areas and its validation in the Strait of Bali. *Proceedings of PORSEC 2014 12th Biennial Conference of Pan Ocean Remote Sensing Conference*. Bali: PAN Ocean Remote Sensing.

Rintaka W. E. & Susilo, E. (2015). Analisis model suhu, klorofil-a, net primary productivity (NPP) kaitannya terhadap jumlah tangkapan lemuru (*Sardinella lemuru*) di perairan Selat Bali (Analysis of temperature, chlorophyll-a, net primary productivity (NPP) in relation to lemuru (*Sardinella lemuru*) catches in the Bali Strait). *Prosiding Simposium Nasional KP II.* Makasar, Indonesia: Universitas Hasanudin.

Sirjacobs, D., Alvera-Azcarate, A., Barth A., & Lacroix, G. (2011). Cloud filling of ocean colour and sea surface temperature remote sensing products over the Southern North Sea by the data interpolating empirical orthogonal functions methodology. *Journal of Sea Research, 65*(1), 114–130.

Suniada, D. (2009) Klasifikasi tutupan awan menggunakan data sensor satelit NOAA/AVHRR APT (Cloud cover classification using NOAA/AVHRR APT imagery). *Proceedings of Seminar on Intelligent Technology and Its Applications*.

Susanto, R. D., Moore, T. S., & Marra, J. (2006). Ocean color variability in the Indonesian Seas during the 16. SeaWiFS era. *An Electronical Journal of the Earth Sciences, Vol.7*(5):), 1-–

Susilo, E. & Suniada K. I. (2015). The suitability of the predicted fishing ground maps (PPDPI) and micronecton biomass. *Proceedings of The 1st International Symposium on Marine and Fisheries Research.*

Walpole, R. E. (1993). *Pengantar Statistika Edisi 3 (Introduction to Statistics 3rd Edition).* Jakarta:PT. Gramedia Pustaka Utama

Widayati, C. S. W. (2009). Komparasi beberapa metode estimasi kesalahan pengukuran (Comparison of several methods of the measurement error estimation). *Jurnal Penelitian dan Evaluasi Pendidikan 13*(2), 182–197.

Yunanto A. & Suniada, K. I. (2008). Korelasai antara hasil tangkapan ikan dan jarak lokasi penangkapan dengan fishing ground peta ppdpi terdekat: Studi kasus data respon balik hasil tangkapan lkan KM. Sumber Rejeki di PPN Pemangkat (Correlation between fish catches and distance of fishing location with closest PPDPI map: Case study of feedback data from KM KM. Sumber Rejeki in PPN

Pemangkat). *Prosiding Bali Scientific Meeting.* ISBN: 978-979-15873-3-4

Zhu, L., Suomalainen, J., Liu, J., Hyyppä, J., Kaartinen, H., & Haggren, H. (2018). A review: Remote sensing sensors. In R. B. Rustamov, S. Hasanova, & M. H. Zeynalova (Eds.), *Multi-purposeful application of geospatial data* (pp. 19–42). London: Books on Demand.

Supplements

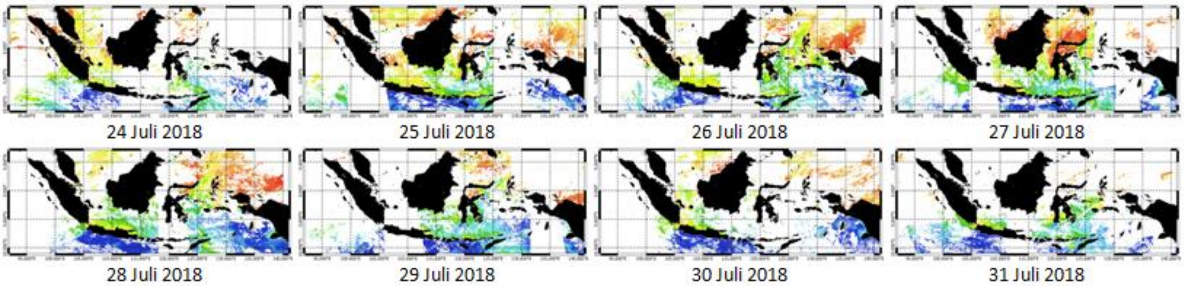

Spatial distribution of 1D mosaic SST data from 24 – 31 July 2018

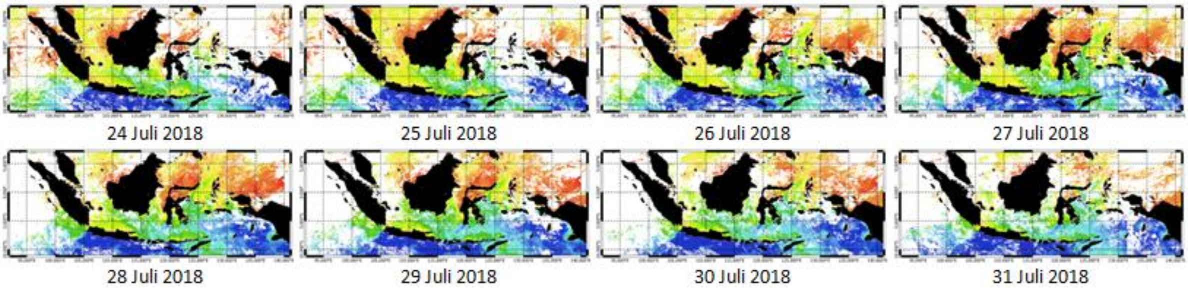

Spatial distribution of 3D mosaic SST data from 24 – 31 July 2018

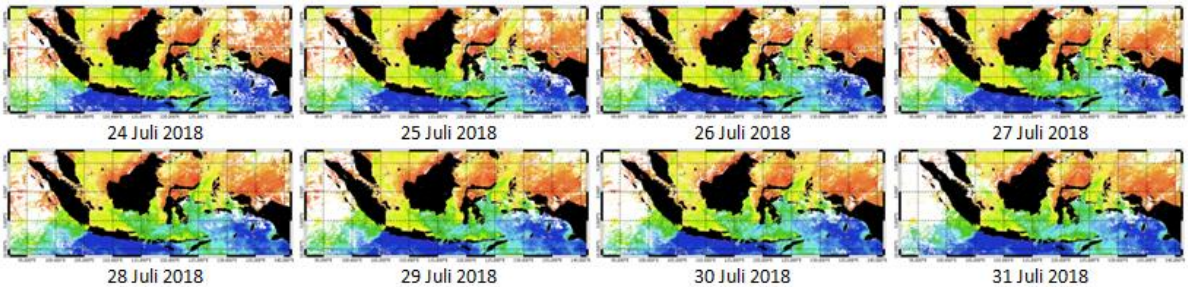

Spatial distribution of 7D mosaic SST data from 24 – 31 July 2018

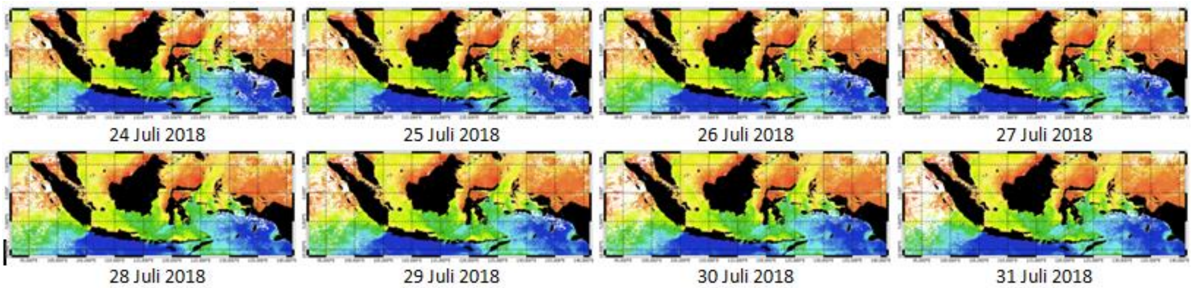

Spatial distribution of 14D mosaic SST data from 24 – 31 July 2018

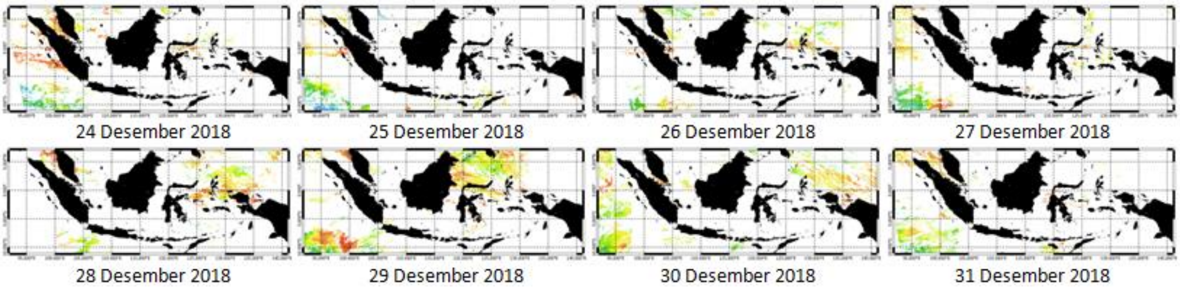

Spatial distribution of 1D mosaic SST data from 24 – 31 December 2018

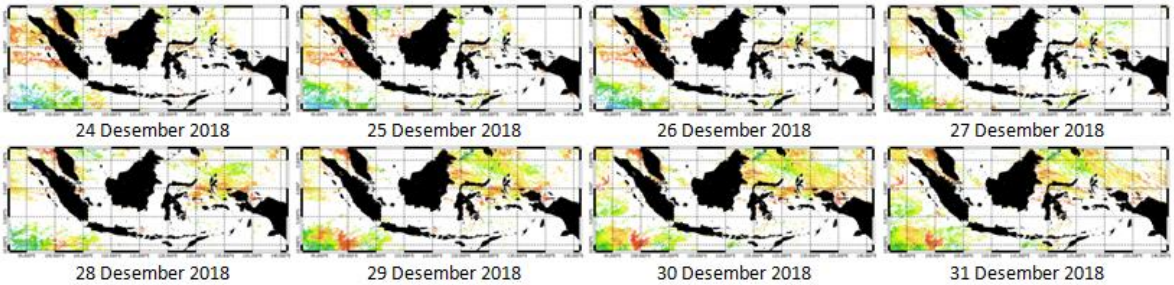

Spatial distribution of 1D mosaic SST data from 24 – 31 December 2018

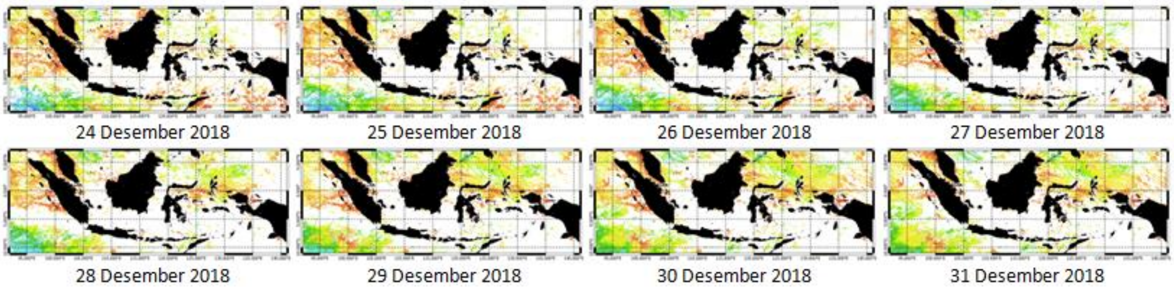

Spatial distribution of 1D mosaic SST data from 24 – 31 December 2018

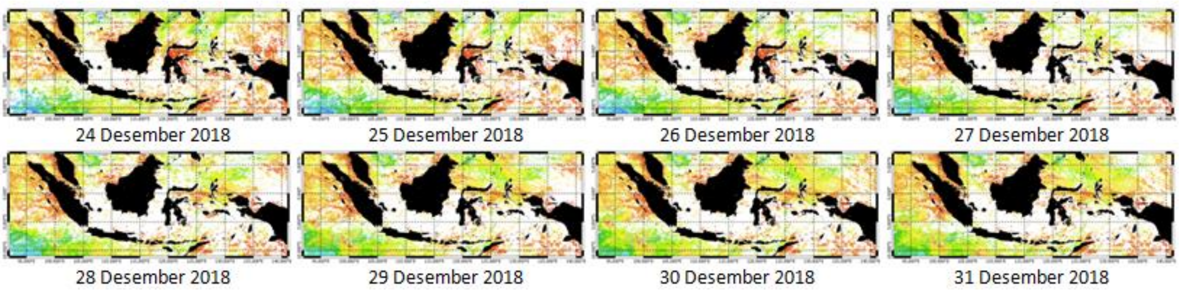

Spatial distribution of 1D mosaic SST data from 24 – 31 December 2018